



# A Large Hadron Electron Collider at CERN

LHeC Study Group <sup>1</sup>

## Abstract

This document provides a brief overview of the recently published report on the design of the Large Hadron Electron Collider (LHeC), which comprises its physics programme, accelerator physics, technology and main detector concepts. The LHeC exploits and develops challenging, though principally existing, accelerator and detector technologies. This summary is complemented by brief illustrations of some of the highlights of the physics programme, which relies on a vastly extended kinematic range, luminosity and unprecedented precision in deep inelastic scattering. Illustrations are provided regarding high precision QCD, new physics (Higgs, SUSY) and electron-ion physics. The LHeC is designed to run synchronously with the LHC in the twenties and to achieve an integrated luminosity of  $O(100) \text{ fb}^{-1}$ . It will become the cleanest high resolution microscope of mankind and will substantially extend as well as complement the investigation of the physics of the TeV energy scale, which has been enabled by the LHC.

Submitted to the Cracow Symposium of the  
Update of the European Strategy for Particle Physics,  
Cracow (Poland) September 2012.

---

<sup>1</sup>For the current author list see the end of this note. Contacts: [oliver.bruning@cern.ch](mailto:oliver.bruning@cern.ch) and [max.klein@cern.ch](mailto:max.klein@cern.ch)

# 1 Introduction - the LHeC on one page

Deep inelastic lepton-hadron scattering (DIS) represents the cleanest probe of partonic behaviour in protons and nuclei. Highest energy electron-parton collisions provide unique information on the physics beyond the Standard Model (SM). The principal aim of the LHeC conceptual design report (CDR) [1] has been to lay out the design concepts for a second generation DIS electron-proton ( $ep$ ), and a first electron-ion ( $eA$ ) collider, taking unique advantage of the intense, high energy hadron beams of the Large Hadron Collider. The LHeC in its default design configuration uses a 60 GeV electron beam of high intensity based on a racetrack, energy recovery configuration using two 10 GeV electron linacs. It thus exceeds the luminosity of HERA by a factor of 100 and reaches a maximum  $Q^2$  of above 1 TeV<sup>2</sup> as compared with a maximum of 0.03 TeV<sup>2</sup> at HERA. Correspondingly the lowest Bjorken  $x$  covered in the DIS region with the LHeC is about  $10^{-6}$ , where gluon saturation is expected to exist. This coverage allows a multitude of crucial DIS measurements to be performed, to complement and extend the search potential for new physics at the LHC, and it also makes the LHeC a testing ground for the Higgs boson cleanly produced in  $WW$  and  $ZZ$  fusion in  $ep$ . The extension of the kinematic coverage in DIS lepton-ion collisions amounts to nearly 4 orders of magnitude and can be expected to completely change the understanding of quark-gluon interactions in nuclei, tightly constraining the initial conditions of the formation of the quark-gluon plasma (QGP). The LHeC project represents a unique possibility to take forward the field of DIS physics as an integral part of the future high energy physics programme. It enhances the exploration of the accelerator energy frontier with the LHC. Naturally it is linked to the LHC time schedule and lifetime, which is estimated to continue for two decades hence. Therefore, a design concept has been presented which uses available, yet challenging, technology, both for the accelerator and for the detector, and time schedules are considered for realising the LHeC within about the next decade.

The CDR [1] describes in considerable detail two options for the LHeC, a ring-ring (RR) and a linac-ring (LR) configuration. In a recent workshop [2] following the publication of the CDR, it was decided to pursue the technical design work for the LR configuration only, keeping the RR as a backup in case new developments suggest to come back to it or if the LR design meets insurmountable problems. For comparison, the main parameters for both the RR and the LR configurations are listed in Table 1. The luminosity is constrained by a chosen wall-plug power limit of 100 MW for the lepton beam. The actual  $e$  beam power consumption is therefore limited to a few tens of MW. The linac option, however, effectively uses almost a GW of beam power by recovering the energy of the spent beam. Both the RR and the LR option are designed to provide  $10^{33} \text{ cm}^{-2} \text{ s}^{-1}$  luminosities. The LR configuration has high electron beam polarisations but realistically has a significantly reduced  $e^+p$  luminosity with respect to  $e^-p$ . To mitigate this limitation, various R&D options are presented in the CDR. The LHeC parameters rely on the so-called ultimate LHC beam configuration. From today's experience with the LHC operation, even more performant proton beam parameters can be expected. It is thus possible that the improved proton beam parameters of the HL-LHC upgrade will lead to a significantly higher luminosity for the LHeC than is quoted here. The first estimates of the luminosity in  $eA$  point to a good basis for low  $x$  electron-ion scattering measurements, even in time-restricted periods of operation. More refined studies are required, in particular for the case of deuterons, which have yet to be used in the LHC. The small beam spot size is particularly well suited for tagging of charm and beauty decays. Backscattered laser techniques can provide a real photon beam derived from the  $e$  linac with rather high efficiency, which would give access to  $\gamma p$  and  $\gamma A$  or even  $\gamma\gamma$  physics at high energies.

Section 2 provides first an extended overview of the LHeC, its physics potential, further details on the accelerator and a suitable detector concept. The section concludes with remarks on the time schedule and on synergies with related developments. In Section 3 the physics programme is illustrated, with a brief physics overview table followed by one-page descriptions of selected key topics: PDFs, low  $x$  and heavy ion physics, supplemented by discussions on the possible importance of the LHeC for the study of the Higgs boson and for searches for supersymmetry (SUSY). The paper concludes with a short comment on the LHeC status and next steps. It relies on the CDR [1] and novel physics, technical and organisational considerations as were presented at the June 2012 CERN-ECFA-NuPECC workshop [2] on the LHeC. The current text replaces the draft version of the paper submitted on July 31, 2012.

electron beam 60 GeV	Ring	Linac
$e^- (e^+)$ per bunch $N_e [10^9]$	20 (20)	1 (0.1)
$e^- (e^+)$ polarisation [%]	40 (40)	90 (0)
bunch length [mm]	6	0.6
tr. emittance at IP $\gamma\epsilon_{x,y}^e$ [mm]	0.59, 0.29	0.05
IP $\beta$ function $\beta_{x,y}^*$ [m]	0.4, 0.2	0.12
beam current [mA]	100	6.6
energy recovery efficiency [%]	—	94
proton beam 7 TeV		
protons per bunch $N_p [10^{11}]$	1.7	1.7
transverse emittance $\gamma\epsilon_{x,y}^p [\mu\text{m}]$	3.75	3.75
collider		
Lum $e^-p (e^+p) [10^{32}\text{cm}^{-2}\text{s}^{-1}]$	9 (9)	10 (1)
bunch spacing [ns]	25	25
rms beam spot size $\sigma_{x,y} [\mu\text{m}]$	45, 22	7
crossing angle $\theta$ [mrad]	1	0
$L_{eN} = A L_{eA} [10^{32}\text{cm}^{-2}\text{s}^{-1}]$	0.45	1

Table 1: Baseline design parameters of the Ring (RR) and the Linac (LR) configurations of the LHeC. The technical design will be pursued for the electron Linac with the Ring as a back-up configuration. The luminosity corresponds to a total wall plug power limit of 100 MW for the electron beam. The LHeC physics programme primarily uses protons but foresees also electron collisions with heavy ions ( $eA$ ) and with deuterons ( $eD$ ).

## 2 An Overview of the LHeC

### 2.1 Physics

#### Cornerstones of the Physics Programme

The LHeC, with a multi-purpose detector, has a unique physics programme of deep inelastic scattering, which can be pursued with unprecedented precision over a hugely extended kinematic range. This comprises a per mille level precision measurement of  $\alpha_s$ , accompanied by ultra-precise charm and beauty density measurements, the accurate mapping of the gluon field over five orders of magnitude in Bjorken  $x$ , from  $x \simeq 3 \cdot 10^{-6}$  up to  $x$  close to 1, the first assumption-free, all-flavour PDFs including first direct measurements of the  $Q^2$  and  $x$  dependences of the strange and top quark distributions, and the resolution of the partonic structure of the photon. Neutron and nuclear structure can be explored in a vast new kinematic region, as these were uncovered by HERA, and high precision electroweak measurements can be made, for example of the scale dependence of the weak mixing angle  $\sin^2 \Theta_W$  and of the light-quark weak neutral current couplings. These and more exclusive measurements of e.g. jets and diffraction at high energy and mass scales, represent new challenges for the development of Quantum Chromodynamics to a new level of precision. By accessing very low  $x$  values, down to  $10^{-6}$  at  $Q^2 \simeq 1 \text{ GeV}^2$ , the LHeC is expected to resolve the question of whether and how partons exhibit non-linear interaction dynamics where their density is particularly high, and whether indeed there is a damping of the rise of the parton densities towards low  $x$ , a question also related to ultra-high energy neutrino physics, which probes  $x$  values as small as  $10^{-8}$ .

#### Relation to QCD: Developments and Discoveries

The ultra-high precision measurements with the LHeC challenge perturbative QCD to be further developed, by preparing for a consistent DIS analysis to N<sup>3</sup>LO. Precision measurements of generalised parton distributions in DVCS are necessary for the development of a parton model theory based on scattering amplitudes and the development of a 3-dimensional view of the proton. Analysis in the extended phase space will pin down the mechanism of parton emission and will determine unintegrated, transverse momentum dependent parton distributions for the description of  $ep$  as well as  $pp$  final states. The coverage of extremely low  $x$

regions at  $Q^2 \geq 1 \text{ GeV}^2$ , both in  $ep$  and in  $eA$ , will establish the basis for the theoretical development of non-linear parton evolution physics. High energy  $ep$  scattering may be important for constructing a non-perturbative approach to QCD based on effective string theory in higher dimensions. Instantons are a basic aspect of non-perturbative QCD, which also predicts the existence of the Odderon, a dressed three-gluon state, and both are yet to be discovered. A new chapter in  $eA$  scattering will be opened with measurements of unprecedented kinematic range and precision, allowing huge progress in the understanding of partonic interactions in nuclei, which is still in its infancy. It will also probe the difference between hadronisation phenomena inside and outside the nuclear medium. The establishment of an ultra-high parton density, “black-body” limit in DIS would change the scaling behaviour of the structure functions and the rates with which diffraction and exclusive vector meson production occur. QCD is a subtle theory which is far from being mastered and many of its areas call for a renewed and extended experimental basis.

## Relations to LHC Physics

Deep inelastic scattering is the ideal process for the determination of the quark and gluon distributions in the proton. Studies of the parton substructure of the nucleon are of great interest for the development of strong interaction theory, but they are also a necessary input for new physics searches and studies at the LHC, whose potential will be correspondingly enhanced. With the increasingly apparent need to cover higher and higher new particle masses in this endeavour, it becomes ever more important to pin down the parton behaviour at large  $x$ , which governs both signal and background rates near to the LHC kinematic limit. An example is the prediction of gluino pair production cross sections from gluon-gluon fusion, which are currently not well known at masses beyond a few TeV, and for which a new level of precision on the gluon distribution will be critical. Similar situations are expected to arise in future studies of electroweak and other new physics, where large  $x$  parton distributions will play a crucial role. QCD predicts factorisation as well as resummation phenomena which can be tested with much enhanced sensitivity by combining LHC and LHeC results in inclusive and also in diffractive scattering. Certain parton distribution constraints, e.g. for the strange quark, are also derived from Drell-Yan measurements of  $W$  and  $Z$  production at the LHC, which will be verified with much extended range, accuracy and completeness at the LHeC. The  $eA$  measurements determine the parton densities and interaction dynamics in nuclei and are therefore a natural and necessary complement to the  $AA$  and  $pA$  investigations made with the LHC.

Depending on what new phenomena are found at the LHC, which has a superior cms energy compared to the LHeC (and to any of the proposed  $e^+e^-$  colliders), there are various scenarios where the cleaner  $ep$  initial state can help substantially to clarify and to investigate new physics. Key examples are the spectroscopy of leptoquarks,  $R$ -parity violating SUSY states, substructure and contact interaction phenomena, as well as the search for excited electron or neutrino states.

The Higgs particle is produced in  $WW$  and  $ZZ$  fusion in  $ep$  collisions at the LHeC. These production modes can be uniquely identified by the nature of the charged or neutral current process, and decays can be studied with low background, including the dominant decay to  $b\bar{b}$  to about 4 % precision. From the  $WW$  production the contributions from CP even (SM) or odd (non-SM) Higgs quantum numbers can be unfolded.

As the LHC results continue to appear and the LHeC design proceeds, the relation between the two projects will become a more central part of the developments of the physics, the detector and the machine.

## 2.2 Accelerator

### Electron Beam Layout and Civil Engineering

The default electron beam energy is set to 60 GeV, see [1]. Two suitable configurations have been considered in the design report: a storage ring mounted on top of the LHC magnets, the ring-ring configuration (RR), and a separate linac, the linac-ring configuration (LR). In the RR case, bypasses of 1.3 km length each are considered around the existing LHC experiments, also housing the RF. This option is now treated as backup only, mainly because of its strong interference with the LHC. For the LR case, based on available cavity technology and accepting a synchrotron energy loss of about 1 % in the arcs, a new tunnel of racetrack shape

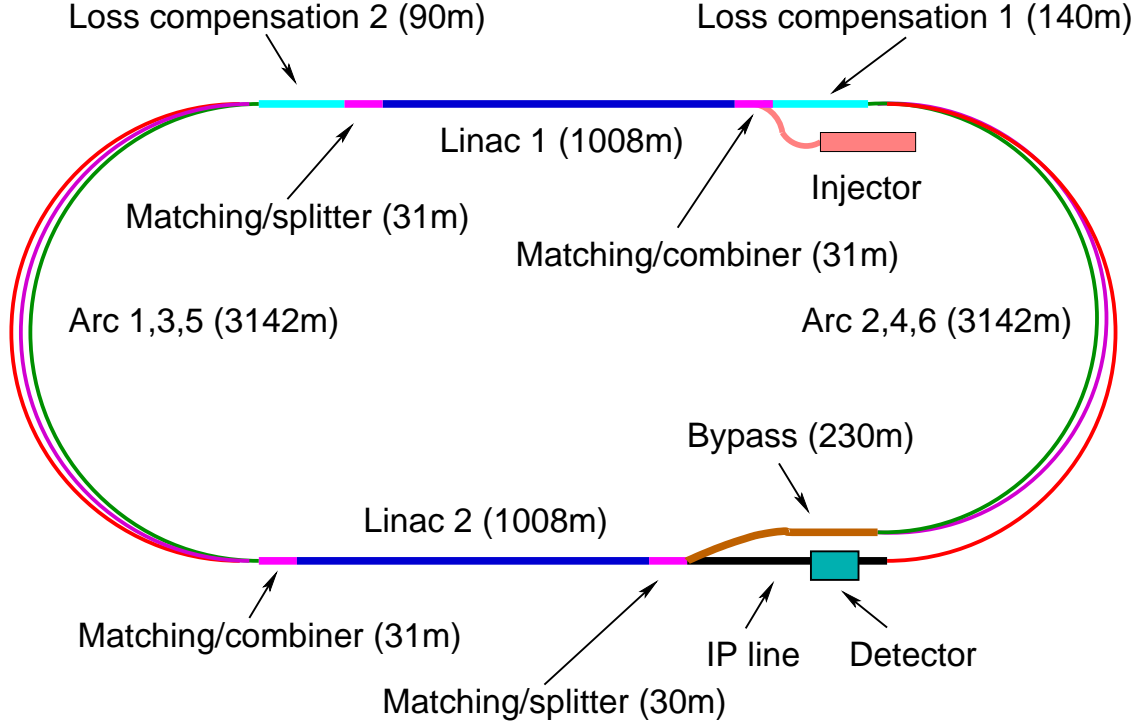


Figure 1: Schematic view on the LHeC racetrack configuration. Each linac accelerates the beam to 10 GeV, which leads to a 60 GeV electron energy at the collision point with three passes through the opposite linear structures of 60 cavity-cryo modules each. The arc radius is about 1 km, mainly determined by the synchrotron radiation loss of the 60 GeV beam which is returned from the IP and decelerated for recovering the beam power. Comprehensive design studies of the lattice, optics, beam (beam) dynamics, dump, IR and return arc magnets, as well as auxiliary systems such as RF, cryogenics or spin rotators are contained in the CDR [1], which as for physics and detector had been reviewed by 24 referees appointed by CERN.

and a length of 9 km is required, not much larger than HERA or the SPS at CERN, see Fig. 1. The tunnel is arranged tangential to IP2 (see below) and is best positioned inside the LHC, which avoids a clash with the LHC injection line TI2 and allows access shafts at the Preveessin and Meyrin sites of CERN, or in close proximity, to be erected. The civil engineering (CE) concepts were evaluated externally and no principal problem has been observed which would prevent completion of a tunnel within a few years time. For the project to begin in the early twenties, the CE efforts are considered to be strengthened by 2013/14.

## Components

Designs of the magnets, RF, cryogenic and further components have been considered in some detail. Some major parameters for both the RR and the LR configurations are summarised in Tab. 2. The total number of magnets (dipoles and quadrupoles excluding the few special IR magnets) and cavities is 4160 for the ring and 5978 for the linac case. The majority are the 3080 (3504) normal conducting dipole magnets of 5.4 (4) m length for the ring (linac return arcs), for which short model prototypes have already been successfully built, testing different magnet concepts, at BINP Novosibirsk and at CERN. The number of high quality cavities for the two linacs is 960, grouped in 120 cavity-cryo modules. The cavities of 1.04 m length are operated at a currently preferred frequency of 721 MHz, at a gradient of about 20 MV/m in CW mode, as is required for energy recovery. The cryogenics system of the ring accelerator is of modest demand. For the linac it critically depends on the cooling power per cavity, which for the draft design is assumed to be 32 W at a temperature of 2 K. This leads to a cryogenics system with a total electric grid power of 21 MW. The projected development of a cavity-cryo module for the LHeC is directed to achieve a high  $Q_0$  value and to reduce the dissipated heat per cavity, which will reduce the dimension of the cryogenics system.

	Ring	Linac
magnets		
number of dipoles	3080	3504
dipole field [T]	0.013 – 0.076	0.046 – 0.264
number of quadrupoles	968	1514
RF and cryogenics		
number of cavities	112	960
gradient [MV/m]	11.9	20
linac grid power [MW]	–	24
synchrotron loss compensation [MW]	49	23
cavity voltage [MV]	5	20.8
cavity $R/Q$ [ $\Omega$ ]	114	285
cavity $Q_0$	–	$2.5 \cdot 10^{10}$
cooling power [kW]	5.4@4.2 K	30@2 K

Table 2: Selected components and parameters of the electron accelerators for the 60 GeV  $e$  beam energy.

## Interaction Region and Choice of IP

Special attention is devoted to the interaction region design, which comprises beam bending, direct and secondary synchrotron radiation, vacuum and beam pipe demands. Detailed simulations are presented in [1] of synchrotron radiation effects, which will have to be pursued further. Stress simulations, geometry and material development considerations are presented for the detector beam pipe, which in the LR case is very asymmetric in order to accommodate the synchrotron radiation fan. The LR configuration requires a long dipole, currently of  $\pm 9$  m length in both directions from the interaction point, to achieve head-on  $ep$  collisions. The dipole has been integrated in the LR detector concept. The IR requires a number of focusing magnets with apertures for the two proton beams and field-free regions through which to pass the electron beam. The field requirements for the RR option (gradient of 127 T/m, beam stay-clear of 13 mm ( $12\sigma$ ), aperture radius of 21 (30) mm for the  $p$  ( $e$ ) beam) allow a number of different magnet designs using proven  $NbTi$  superconductor technology and make use of cable ( $MQY$ ) developments for the LHC. The requirements for the linac are more demanding in terms of field gradient (approximately twice as large) and tighter aperture constraints which may be better realised with  $Nb_3Sn$  superconductor technology, requiring prototyping.

The detector requires an interaction point for  $ep$  collisions while the LHC runs. There are eight points with adjacent long straight tunnel sections, called IP1-IP8, that could in principle be used for an experimental apparatus. Four of these (IP1, IP2, IP5 and IP8) house the current LHC experiments. There is no experimental cavern at IP3 nor IP7, and it is not feasible to consider excavating a new cavern while the LHC operates. Since IP6 houses the beam extraction (dumps) and IP4 is occupied with RF equipment, the LHeC project can only be realised according to the present understanding if it uses one of the current experimental halls. The nature of the  $ep$  collider operation is to run synchronously with  $pp$  in the high luminosity phase of the LHC, which is determined primarily by the searches for ultra-rare phenomena by ATLAS (IP1) and CMS (IP5). A 9 km tunnel excavation and surface installations close to an international airport, as would be required at IP8, is considered not to be feasible. Therefore, IP2 has been used as the reference site for the CDR. IP2 appears to be well suited as it has an experimental surface hall for detector pre-assembly and with the LHeC inside the LHC ring, access to the linacs seems to be possible with shafts and surface installations placed on, or very close to existing CERN territory. It therefore has to be tentatively recognised that IP2 is in practice the only option for housing the LHeC detector. This would require a transition from the ALICE to the LHeC detector, for which consultations between ALICE and LHeC have recently been initiated.

The LHeC design report considers only one detector. This could possibly be built by two analysis collaborations, cooperating in its operation but otherwise ensuring independent and competing software and analysis approaches, as a “push-pull” detector philosophy is not feasible.

## 2.3 Detector

The physics programme depends on a high level of precision, required for example for the measurement of  $\alpha_s$ , and on the reconstruction of complex final states, as appear in charged current single top events or in Higgs production and decay into  $b$  final states. The detector acceptance has to extend as close as possible to the beam axis because of the interest in the physics at small and large Bjorken  $x$ . The dimensions of the detector are constrained by the radial extension of the beam pipe, in combination with maximum polar angle coverage, down to about  $1^\circ$  and  $179^\circ$  for forward going final state particles and backward scattered electrons at low  $Q^2$ , respectively. A cross section of the central, baseline detector is given in Fig. 2. In the central barrel, the

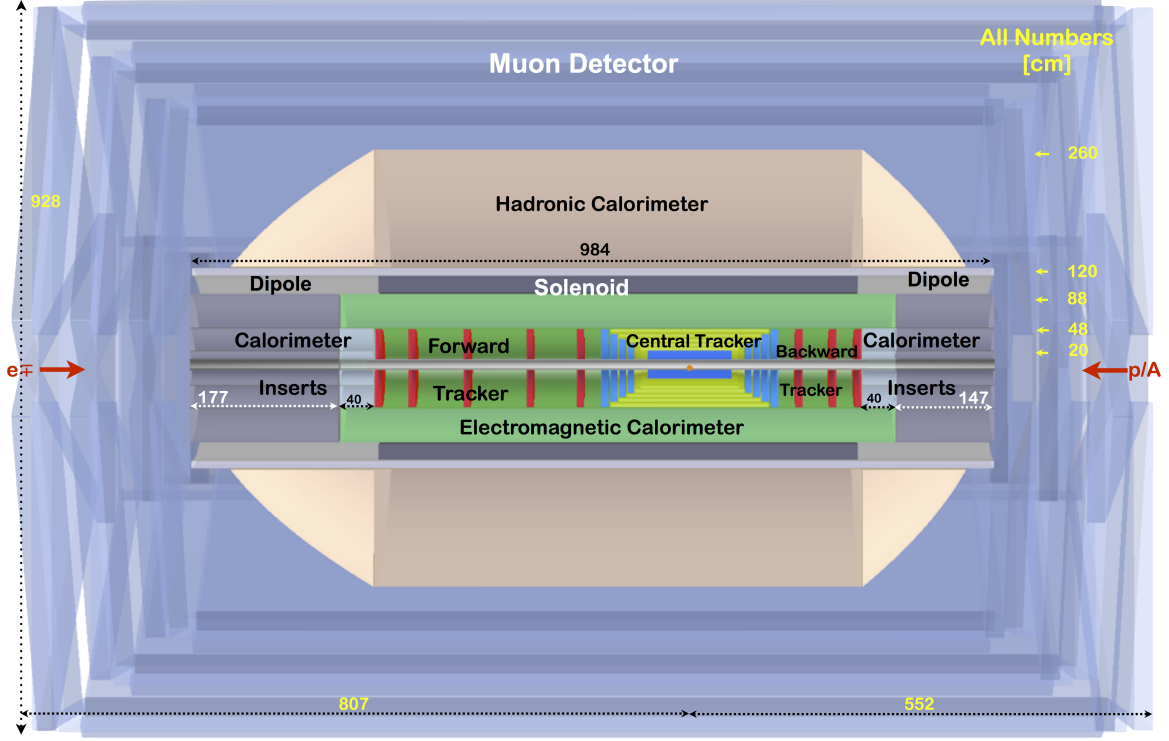


Figure 2: An  $rz$  cross section of the LHeC detector in its baseline design with the magnet configuration for LR, with the solenoid and dipoles placed between the electromagnetic and the hadronic calorimeters. The proton beam, from the right, collides with the electron beam, from the left, at the IP which is surrounded by a central tracker system, complemented by large forward and backward tracker telescopes, and followed by sets of calorimeters. The detector dimensions are  $\approx 13.6$  m in  $z$  and a diameter of  $\approx 9.3$  m, which fits in the L3 magnet structure considered for supporting the LHeC apparatus [1].

following detector components are currently considered: a central silicon pixel detector surrounded by silicon tracking detectors of strip or possibly strixel technology; an electromagnetic LAr calorimeter inside a 3.5 T solenoid and a dipole magnet required to achieve head-on collisions; a hadronic tile calorimeter serving also for the solenoid flux return; a muon detector, so far only used for muon identification, relying on the precise inner tracking for muon momentum measurements. The electron at low  $Q^2$  is scattered into the backward silicon tracker and its energy is measured in backward calorimeters. In the forward region, components are placed for tracking and for calorimetry to precisely reconstruct jets over a wide energy range up to  $O(\text{TeV})$ . Simulations of tracking and calorimeter performance are used to verify the design, although a complete simulation is not yet available. The report also contains designs for forward and backward tagging devices for diffractive and neutron physics and for photoproduction and luminosity determinations, respectively. The time schedule of the LHeC project demands a detector to be ready within about ten years. The radiation level at the LHeC is lower than in  $pp$ , and the  $ep$  cross section is low enough for the experiment not to suffer

from pile-up, which are the two most demanding constraints for the ATLAS and CMS detector upgrades for the HL-LHC. The choice of components for the LHeC detector can rely on the experience obtained at HERA, at the LHC, including its detector upgrades currently being developed, and also on detector development studies for the ILC. The detector development, while requiring prototyping, may yet proceed without an extended R&D program.

A first study has been made about the principles of pre-mounting the detector at the surface, lowering and installing it at IP2. The detector is small enough to fit into the L3 magnet structure of 11.2 m diameter, which is still resident in IP2 and is available as mechanical support. Based on the design, as detailed in the CDR, it is estimated that the whole installation can be done in 30 months, which is compliant with the operations currently foreseen in the LS3 shutdown, during which ATLAS intends to replace its complete inner tracking system.

## Time Schedule and Mode of Operation

The electron accelerator and new detector require a period of about a decade to be realised, based on experience from previous particle physics experiments. This duration fits with the industrialisation and production schedules, mainly determined by the required  $\sim 3500$  approximately 5 m long warm arc dipoles and the 960 cavities for the Linac. The current lifetime estimates for the LHC predict two more decades of operation. An integrated luminosity for the LHeC of  $O(100) \text{ fb}^{-1}$  may be collected in about one decade. This and the current shutdown planning of the LHC define the basic time schedule for the LHeC project: it has to be installed during the long shutdown LS3 of the LHC, currently scheduled for 2022 and a period of about 2 years. The connection of the electron and proton beams and the detector installation can be realised in a period not significantly exceeding this tentative time window. The considerations of beam-beam tune shifts show that the  $ep$  operation may proceed synchronously with  $pp$ . Therefore with the electron beam, the LHC will be turned into a three beam facility. In the design considerations [1] it has been excluded to operate  $ep$  after the  $pp$  programme is finished, a) because this would make the LHeC as part of the LHC much more expensive by adding an extra decade of LHC operation requiring also substantial efforts to first consolidate the LHC, when the high radiation  $pp$  programme is over, and b) since one would lose the intimate and possibly crucial connection between the  $ep/pp$  and the  $eA/AA$  physics programmes, as sketched in this note.

## 2.4 Synergies

The LHeC represents a natural extension to the LHC, offering maximum exploitation of the existing LHC infrastructure at CERN. This is a unique advantage as compared to when HERA was built, for example. Physics-wise it is part of the exploration of the high energy frontier and as such linked to the LHC and the lepton-lepton colliders under consideration, a relation which resembles the intimate connection of HERA to the physics at Tevatron and LEP for the investigation of physics at the Fermi scale. As an  $ep$  and  $eA$  machine, the LHeC unites parts of the particle and nuclear physics communities for a common big project. It has a characteristic electroweak, QCD and nucleon structure physics programme which is related primarily to the LHC but also to lower energy fixed target DIS experiments operating at CERN and Jlab, and also to plans for realising lower energy electron-ion colliders at BNL and at Jlab. The superconducting (SC) IR magnets resemble HL-LHC superconducting magnet developments by the USLARP and SC magnet developments elsewhere. The LHeC linac is relevant to a variety of projects such as the XFEL at DESY, ESS, the CEBAF upgrade at Jlab, the SPL at CERN and other projects for high quality cavity developments. Through the development of its high energy ERL application to particle physics, the LHeC is related to about ten lower energy projects worldwide, which are developing the energy recovery concept. The detector technology is linked mainly to the LHC experiments and some of their upgrades. It is thus evident that there are very good prospects for realising the LHeC within dedicated international collaborations at a global scale where mutual benefits can be expected at many levels. The dimension of the LHeC and the technologies involved make it a suitable project for particle physics to develop and expand its collaboration with industry.



### 3 Physics Highlights of the LHeC

#### 3.1 Summary of the Physics Programme

The LHeC represents a new laboratory for exploring a hugely extended region of phase space with an unprecedented high luminosity in high energy DIS. It is the link between the LHC and a future lepton collider fulfilling the role played by HERA with the Tevatron and LEP, but with much higher precision in an extended kinematic range. Its physics is fundamentally new, and it is also complementary especially to the LHC, for which the electron beam is an upgrade. It addresses a broad range of physics questions and an attempt for a schematic overview on the LHeC physics programme as seen from today's perspective is presented in Tab.3. The conquest of new regions of phase space and intensity has often lead to surprises, which tend to be difficult to tabulate.

QCD Discoveries	$\alpha_s < 0.12$ , $q_{sea} \neq \bar{q}$ , instanton, odderon, low $x$ : (n0) saturation, $\bar{u} \neq \bar{d}$
Higgs	$WW$ and $ZZ$ production, $H \rightarrow b\bar{b}$ , $H \rightarrow 4l$ , CP eigenstate
Substructure	electromagnetic quark radius, $e^*$ , $\nu^*$ , $W^?$ , $Z^?$ , top?, $H^?$
New and BSM Physics	leptoquarks, RPV SUSY, Higgs CP, contact interactions, GUT through $\alpha_s$
Top Quark	top PDF, $xt = x\bar{t}^?$ , single top in DIS, anomalous top
Relations to LHC	SUSY, high $x$ partons and high mass SUSY, Higgs, LQs, QCD, precision PDFs
Gluon Distribution	saturation, $x \approx 1$ , $J/\psi$ , $\Upsilon$ , Pomeron, local spots?, $F_L$ , $F_2^c$
Precision DIS	$\delta\alpha_s \simeq 0.1\%$ , $\delta M_c \simeq 3\text{ MeV}$ , $v_{u,d}$ , $a_{u,d}$ to 2 – 3 %, $\sin^2 \Theta(\mu)$ , $F_L$ , $F_2^b$
Parton Structure	Proton, Deuteron, Neutron, Ions, Photon
Quark Distributions	valence $10^{-4} \lesssim x \lesssim 1$ , light sea, $d/u$ , $s = \bar{s}^?$ , charm, beauty, top
QCD	N <sup>3</sup> LO, factorisation, resummation, emission, AdS/CFT, BFKL evolution
Deuteron	singlet evolution, light sea, hidden colour, neutron, diffraction-shadowing
Heavy Ions	initial QGP, nPDFs, hadronisation inside media, black limit, saturation
Modified Partons	PDFs “independent” of fits, unintegrated, generalised, photonic, diffractive
HERA continuation	$F_L$ , $xF_3$ , $F_2^{\gamma Z}$ , high $x$ partons, $\alpha_s$ , nuclear structure, ..

Table 3: Schematic overview on key physics topics for investigation with the LHeC.

#### 3.2 Parton Distributions and the Strong Coupling Constant

Despite a series of deep inelastic scattering experiments with neutrinos, electrons and muons using stationary targets and with HERA, and despite the addition of some Drell-Yan data, the knowledge of the various quark distributions in the proton is still limited. Due to the wide kinematic range, huge luminosity, and possibility of beam variations, the LHeC will provide the necessary constraints on all parton (quark and gluon) distributions to determine PDFs completely, free of conventional QCD fit assumptions, which has hitherto not been possible. For example, the valence quarks can be measured up to low and high  $x$ , and the heavy quark distributions,  $xs$ ,  $xc$ ,  $xb$  and  $xt$ , can be determined from dedicated  $c$  and  $b$  tagging analyses with unprecedented precision, all for the first time. The QCD fits, which will necessarily evolve with real LHeC data, will correspondingly be set-up with a massively improved and better constrained, flavour separated input data base, including precision electroweak effects, cf. Fig. 3 (left). This will have a direct impact on the extension of the search range at the LHC at high masses, above a few TeV, see Sect. 3.6.

From a full simulation of experimental systematic uncertainties, as is described in [1], one concludes that the strong coupling constant  $\alpha_s(M_Z^2)$  can be measured to per mille precision, as compared to a per cent level nowadays. Such a measurement puts the attempts to unite the couplings at the Planck scale on a firm footing for the first time, see Fig. 3 (right). Combined with a similarly high accuracy from jet data, this measurement will eventually resolve the question of whether inclusive DIS and jet-based  $\alpha_s$  measurements lead to the same or to different strong coupling constants. It also finally makes the BCDMS measurement redundant, which for a long time pointed to a very small value of  $\alpha_s$  obtained in the most precise measurement in DIS. The

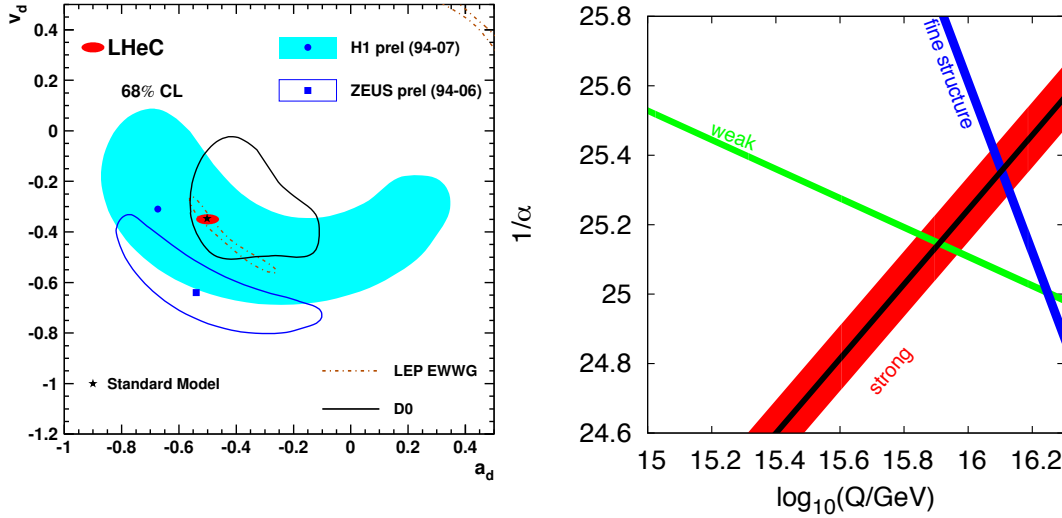


Figure 3: Precision electroweak and strong interaction coupling determinations with the LHeC. Left: Total experimental uncertainty of the vector and axial-vector NC down-quark couplings from the LHeC (red ellipse) compared to present determinations from HERA, Tevatron and LEP; Right: Extrapolation of the coupling constants ( $1/\alpha$ ) within SUSY (CMSSM40.2.5) [4] to the Planck scale. The width of the red line is the uncertainty of the world average of  $\alpha_s$ , which is dominated by the lattice QCD calculation chosen for the PDG average. The black band is the LHeC projected experimental uncertainty [1].

LHeC  $\alpha_s$  measurement is not just a single experiment but represents a whole programme, which renews the physics of DIS and revisits the scale uncertainties in pQCD at the next-to-next-to-next-to leading order level. The LHeC itself provides the necessary basis for such a programme, mainly with a complete set of high precision PDF measurements, including for example the prospect to measure the charm mass to 3 MeV as compared to 30 MeV at HERA (from  $F_2^{cc}$ ), and with the identification of the limits of applicability of DGLAP QCD by discovering or rejecting saturation of the gluon density.

### 3.3 Low $x$ Physics

The parton densities extracted from HERA data exhibit a strong rise towards low  $x$  at fixed  $Q^2$ . The low  $x$  regime of proton structure is a largely unexplored territory whose dynamics are those of a densely packed, gluon dominated, partonic system. It offers unique insights into the gluon field which confines quarks within hadrons and is responsible for the generation of most of the mass of hadrons. Understanding low  $x$  proton structure is also important for the precision study of cosmic ray air showers and ultra-high energy neutrinos and may be related to the string theory of gravity. The most pressing issue in low  $x$  physics is the need for a mechanism to tame the growth of the partons, which, from very general considerations, is expected to be modified in the region of LHeC sensitivity. There is a wide, though non-universal, consensus, that non-linear contributions to parton evolution (for example via gluon recombinations  $gg \rightarrow g$ ) eventually become relevant and the parton densities ‘saturate’. The LHeC offers the unique possibility of observing these non-perturbative dynamics at sufficiently large  $Q^2$  values for weak coupling theoretical methods to be applied, suggesting the exciting possibility of a parton-level understanding of the collective properties of QCD. A two-pronged approach to mapping out the newly accessed LHeC low  $x$  region is proposed in [1]. On the one hand, the density of partons can be increased by overlapping many nucleons in  $eA$  scattering (see next section). On the other hand, the density of a single nucleon source can be increased by probing at lower  $x$  in  $ep$  scattering. Many observables are considered in [1], from which two illustrative examples are chosen here.

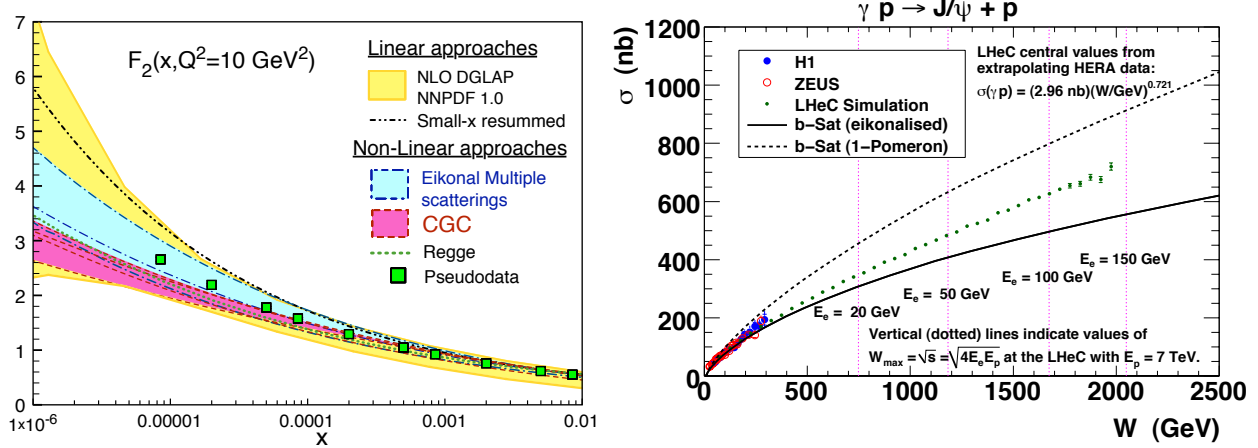


Figure 4: Left: Simulated low  $x$  LHeC  $F_2$  data at a single illustrative value of  $Q^2$ , compared with predictions from standard ‘linear’ DGLAP-based QCD and from models which include saturation effects. Right: Simulated LHeC measurements of the exclusive  $J/\psi$  photoproduction cross section, compared with models which include or neglect saturation phenomena.

Fig. 4 (left) shows simulated low  $x$  LHeC  $F_2$  data at a single example value of  $Q^2$ , compared with three bands of predictions. The ‘NNPDF 1.0’ band is one estimate of the range of variations possible from low  $x$  extrapolations of current NLO DGLAP QCD fits. The ‘Eikonal Multiple scatterings’ and ‘CGC’ bands are envelopes spanning numerous predictions based on two different QCD-based approaches to the onset of non-linear dynamics and parton saturation. It is clear that the LHeC data are more than adequate to distinguish between these different models, particularly when complementary precision data on the  $F_L$  structure function (not shown here, see [1]) are also included. Fig. 4 (right) shows simulated LHeC measurements of the cross section for the exclusive photoproduction of  $J/\psi$  mesons ( $\gamma p \rightarrow J/\psi p$ , obtained as the  $Q^2 \rightarrow 0$  limit of the process  $ep \rightarrow eJ/\psi p$ ), as a function of the  $\gamma p$  centre of mass energy,  $W$ . The ‘b-Sat (1-Pomeron)’ and ‘b-Sat (eikonalised)’ curves correspond to predictions constrained by HERA data which either neglect or include saturation effects, respectively. The conclusion is that LHeC data will not only unambiguously establish the onset of saturation phenomena, but will be highly sensitive to the, presumably rich, underlying dynamics. Moreover, the extraction of generalised Parton Distributions (GPDs) - for both quarks and gluons - accessible in hard exclusive reactions such as deeply virtual Compton scattering and meson electroproduction will allow to understand proton structure in a new, three-dimensional way.

### 3.4 Electron-Ion Scattering

The LHeC will give access to a completely new kinematic regime in the  $x - Q^2$  plane, compared to previous experimental facilities, for exploration of nuclear structure and dynamics of nuclear collisions. As illustrated in Fig. 5 (left), the gain towards smaller  $x$  and larger  $Q^2$  is almost four orders of magnitude. Besides, the  $eA$  mode offers the possibility of a two-pronged approach to explore the small- $x$  dynamics of QCD, where a novel regime, characterised by the breakdown of linear fixed-order perturbation theory applicable in a dilute parton region, and the appearance of non-linear evolution phenomena and saturation of partonic densities, is expected to exist. With all these features being triggered by an increase of parton densities, at the LHeC this novel regime can be approached, as shown in Fig. 5 (right), through a decrease in  $x$  and through an increase in the number of nucleons,  $A$ , involved. The latter can be achieved in  $eA$  collisions both increasing  $A$  and decreasing the impact parameter of the collision - thus the effective number of nucleons involved. For this reason, the physics case presented in [1] for  $ep$  collisions has been made in parallel for  $eA$  whenever possible. As shown in [1, 2], the possibilities for nuclear studies at the LHeC are vast:

- Structure function measurements and their flavour decompositions in  $eA$  will allow nuclear parton densities at small  $x$  to be measured for the first time, testing current extractions through linear evolution equations,

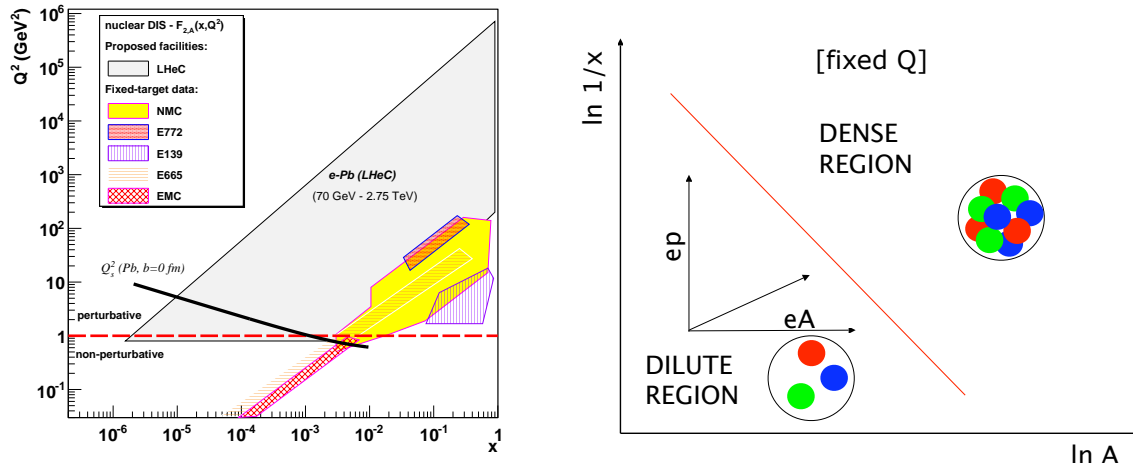


Figure 5: Left: kinematic coverage of the LHeC in the  $\ln Q^2 - \ln 1/x$  plane for nuclear beams, compared with existing nuclear DIS and Drell-Yan experiments. The thick black line locates roughly the expected transition region between a dilute partonic regime above and a dense regime below. Right: schematic view of the different regions for the parton densities in the  $\ln 1/x - \ln A$  plane, for fixed  $Q^2$ . Lines of constant occupancy of the hadron are parallel to the diagonal line shown.

particularly for the presently almost unconstrained gluon density for  $x < 10^{-2}$ , and the unknown charm and beauty densities in nuclei.

- Exclusive vector meson production in  $eA$  will offer a handle, complementary to  $ep$ , on the possible evidence of non-linear dynamics and saturation of partonic densities, as these effects increase with  $A$ .
- Inclusive diffraction in  $eA$  will be measured for the first time, with the possibility of extracting diffractive parton densities in nuclei, and of looking for signals of novel high-density phenomena which are expected to affect diffraction to a larger extent than inclusive observables.
- The dynamics of hadronisation and QCD radiation will be clarified in  $eA$  collisions through semi-inclusive measurements of both particles and jets, of which large yields will be produced up to high transverse momenta. The effects of the nuclear environment will be explored through the modification of yields, hadrochemistry, jet substructure, etc., compared to equivalent  $ep$  measurements.

All these measurements will settle the role of factorisation, either the standard collinear one or some other version suitable for high energies and dense regimes, in  $eA$  collisions for inclusive, semi-inclusive and diffractive observables. Finally, note the strong implications of the investigation of  $eA$  collisions at the LHeC on ultrarelativistic heavy-ion physics, both by constraining the initial state, which is crucial for the quantitative understanding of the subsequent behaviour of the produced medium, and for our understanding of the ability of hard probes to characterise it. Some of these aspects will be explored in  $pA$  collisions at the LHC in a similar kinematical region, but they will be studied at the LHeC in a much cleaner manner.

### 3.5 Higgs Physics with the LHeC

In the Standard Model, the breaking of the electroweak  $SU(2)_L \times U(1)_Y$  symmetry gives mass to the electroweak gauge bosons via the Brout-Englert-Higgs mechanism while the fermions obtain their mass via Yukawa couplings with a scalar Higgs field. With the observation of a Higgs-like boson by the ATLAS and CMS collaborations with a mass around 126 GeV, a new research field has opened in particle physics. The measurement of the couplings of the newly found boson to the known fundamental particles will be a crucial test of the SM and a window of opportunity to establish physics beyond the SM.

At the LHeC, a light Higgs boson could be uniquely produced and cleanly reconstructed either via  $HZZ$  coupling in neutral current (NC) DIS or via  $HWW$  coupling in charged current (CC) DIS. Those vector boson fusion processes have sizeable cross sections, O(100) fb for 126 GeV mass, and they can be easily distinguished, which is a unique advantage in comparison to the VBF Higgs production in  $pp$  scattering. The observability

of the Higgs boson signal at the LHeC was investigated in the CDR [1] initially using the dominant production and decay mode, i.e. the CC reaction  $e^-p \rightarrow H(\rightarrow b\bar{b}) + \nu + X$ , for the nominal 7 TeV LHC proton beam and electron beam energies of 60 and 150 GeV. Signal and multi-jet background processes are generated using MadGraph. The generated events are passed through a custom-made Pythia program version for fragmentation and hadronisation. The event reconstruction is still based on a parameterised, generic LHC-style detector. Very good tracking and  $b$ -tagging capabilities are crucial for the signal identification and enrichment, while a good hadronic energy and flow resolution is important for the background rejection and the tagging of very forward jets. Simple and robust cuts are identified and found to reject effectively e.g. the dominant single-top background, as opposed to refined event weighting and network techniques presently utilised in complex final state (top and Higgs) physics at the LHC, providing an excellent S/B ratio of about 1 at the LHeC. At the default electron beam energy of 60 GeV, for 80 %  $e^-$  polarisation and an integrated luminosity of  $100 \text{ fb}^{-1}$ , the  $Hb\bar{b}$  coupling is estimated to be measurable with a statistical precision of about 4 %, which is not far from the theoretical uncertainty <sup>2</sup>. Typical coupling measurements, such as  $\gamma\gamma$  or  $4l$ , can be made with about 10 % precision with the HL-LHC, while the specific  $b\bar{b}$  coupling will be particularly difficult to measure due to high combinatorial backgrounds in  $pp$ .

It has also been observed, that the LHeC can specifically explore well the CP structure of the  $HWW$  coupling by separating it from the  $HZZ$  coupling and the other signal production mechanisms. Any determination of an anomalous  $HWW$  vertex will thus be free from possible contaminations of these. A further advantage of the  $ep$  collider kinematics stems from the ability to disentangle clearly the direction of the struck parton and the final state lepton (clear definition of forward and backward directions). Compared to the  $pp$  situation,  $ep$  lacks the complications due to underlying event and pile-up driven backgrounds.

The few initial studies performed so far will be pursued further in the light of recent observations from the LHC experiments. For the projected analyses, this primarily concerns using a full LHeC detector simulation, and optimising further the detector design. For the accelerator design it is obvious that a luminosity in excess of  $10^{33} \text{ cm}^{-2}\text{s}^{-1}$  is very desirable. This would open up the possibility of also making precision measurements of rarer ( $\tau$ ,  $Z$ ,  $W$ , perhaps photon) decay channels, the CP angular distributions for both the  $HWW$  and  $HZZ$  couplings, and NC initiated production, a scenario in which the LHeC collider would have a truly remarkable potential to study both the Higgs boson and mechanism.

### 3.6 The Search for SUSY and the LHeC

Supersymmetry (SUSY) is a compelling theory providing an extension of the Standard Model (SM) at arbitrarily high energies. In the SM, the Higgs boson mass suffers from large quantum loop corrections, as large as the cut-off scale of the theory, requiring a high degree of fine-tuning of parameters in order to be cancelled. In SUSY, the addition of supersymmetric partner particles to the known fermions and bosons cancels the largest of these loop effects, permitting the Higgs boson mass to lie naturally at the  $\sim 100 \text{ GeV}$  scale. Supersymmetric models present other advantages, including improved unification of running coupling constants at the Planck scale, see Sect. 3.2, and renormalisation group equations that radiatively generate the scalar potential that leads to electroweak symmetry breaking.

The possible conservation of  $R$ -parity, a discrete quantum number which relates spin ( $S$ ), baryon and lepton numbers ( $B$  and  $L$ ), is fundamental in determining the phenomenology of SUSY. In the framework of generic  $R$ -parity conserving supersymmetric extensions of the SM, SUSY particles are produced in pairs and the lightest supersymmetric particle (LSP) is stable. In a large variety of models the LSP is the lightest neutralino,  $\tilde{\chi}_1^0$ , one of the SUSY partners of the gauge bosons together with its three heavier mass eigenstates ( $\tilde{\chi}_{2,3,4}^0$ ) and the charginos ( $\tilde{\chi}_{1,2}^\pm$ ). The lightest neutralino only interacts weakly and provides a Dark Matter candidate with the appropriate relic density to explain the cosmological Dark Matter. The possible appearance of  $R$ -parity-violating couplings, and hence the non-conservation of baryon and lepton numbers ( $B$  and  $L$ ) in supersymmetric theories, imply an even richer phenomenology. Although  $R$ -parity-violating interactions must be sufficiently small, their most dramatic implication is the automatic generation of neutrino

---

<sup>2</sup> It is worth emphasising that many of these uncertainties, as the parametric ones discussed in [5], are of PDF and QCD nature and therefore will be very much reduced by the results anticipated with the realisation of the LHeC programme. This should contribute significantly to improving the accuracy of the Higgs measurements with the LHC.

masses and mixings. The possibility that the results of atmospheric and solar neutrino experiments may be explained by neutrino masses and mixings originating from  $R$ -parity-violating interactions has motivated a large number of studies and models.

The discovery (or exclusion) of supersymmetric particles remains a high priority for the LHC experiments, the LHC being the primary machine to search for physics beyond the SM at the TeV scale. The role of the LHeC is to complement and possibly resolve the observation of new phenomena. At  $ep$  colliders, SUSY particles could be produced due to sizeable lepton flavour violating terms or, in the framework of  $R$ -parity conserving models, via associated production of selectrons and first and second generation squarks. The latter process would present a sizeable cross section only if the sum of selectron and squark masses is below or around 1 TeV (thus, for relatively light squarks). Current exclusion limits set by the ATLAS and CMS experiments on first and second generation squarks are up to 1.5 TeV under the assumption that the first two squark families are degenerate. In models where this condition is relaxed, windows of discovery relevant for the LHeC might still be open at the time of start-up.

Less stringent constraints exist in the context of  $R$ -parity violating scenarios. Processes of interest for  $ep$  colliders include leptoquark-like processes and associated production of quark-neutralinos via squark-quark-neutralino couplings, where squarks can be off-shell and thus beyond direct LHC exclusion limits. While stringent constraints exist for associated production of leptons and quarks possibly deriving from squark decay, processes of the kind  $eu \rightarrow d\tilde{\chi}_1^0$  and subsequent decays of  $\tilde{\chi}_1^0$  to leptons and quarks might be difficult to study at the LHC, due to the overwhelming SM multi-jet background, and can be successfully searched for at the LHeC.

The LHeC will also provide indirect handles for the case of supersymmetry. The dominant SUSY production channels at the LHC are assumed to be squark-(anti)squark, squark-gluino, and gluino-gluino pair production. All gluon-initiated processes suffer from very large uncertainties due to the extremely limited knowledge of the gluon density at high  $x$ . If gluinos of 2 – 4 TeV mass exist, their discovery, e.g. through enhanced multi-jet production rates (with or without missing transverse momentum) compared with SM predictions, and their kinematic characterisation will depend on the capability to predict their production cross section with good precision. Current PDF fits suffer from very large uncertainties, as shown in Fig. 6 (left), and also differ considerably in their central predictions. This will be completely changed with the high precision LHeC measurements, which will allow for the first time assumption-free, all-flavour PDFs, implying improvements in both the agreement between the range of possible central values as well as the precision. The improvement in the precision of the gluon is illustrated in Fig. 6 (right), while the improvements for the quarks at high  $x$  can be found in [1]. The interest in  $R$ -parity violating SUSY translates directly into the striking potential of the LHeC to determine the lepto-quark or lepto-gluon quantum numbers should such states be discovered at the LHC. The  $ep$  machine has a clean  $s$ -channel single production mode, with variable input beam parameters while the LHC produces them predominantly in pairs. This is discussed in detail in [1], along with the reach in contact interactions, excited leptons, anomalous lepton-quark interactions and other BSM topics.

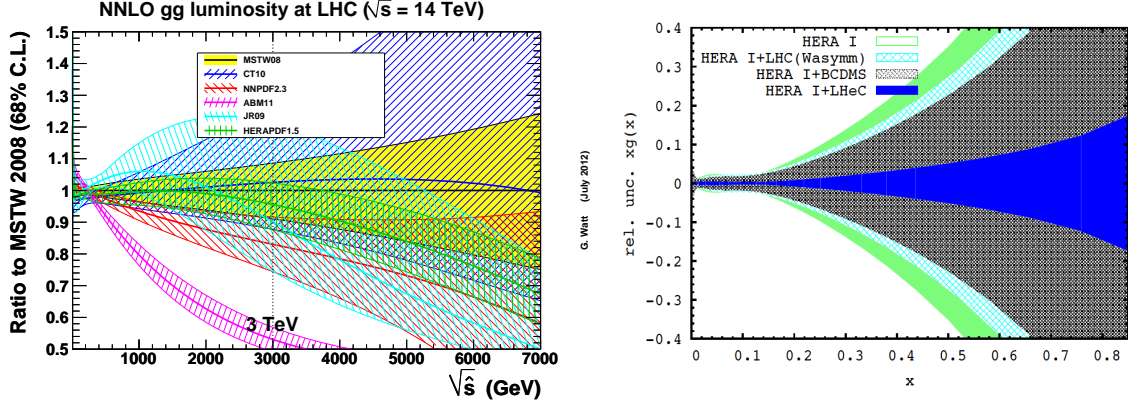


Figure 6: Left: Gluon-gluon luminosity calculated as a function of  $\sqrt{\hat{s}} = \sqrt{x_1 x_2 s}$ , where  $x_1 x_2$  is the product of the two Bjorken  $x$  values with which the two gluons are emitted. The maximum mass one can pair produce is  $M_{\tilde{g}} = \sqrt{x_1 x_2 s}/2$ , i.e. a 4 TeV mass corresponds to an average  $x = \sqrt{x_1 x_2}$  of about 0.6. The  $gg$  luminosity, is a measure, here expressed as the ratio to the MRST08 prediction, of the gluino-pair production process  $gg \rightarrow g \rightarrow \tilde{g}\tilde{g}$ , which is one of the interesting SUSY channels open for discovery, with masses as high as about 4 TeV accessible in the HL-LHC phase. Right: The LHeC will determine the partons at high  $x$  very accurately, together with the strong coupling to per mille precision, which is demonstrated here with the projected uncertainty estimated for the gluon distribution at high  $x$  from inclusive DIS alone (right plot), quoted at the starting scale of the evolution.

## 4 Outlook

The design report [1] shows that the LHeC can be realised at CERN and would substantially enrich the physics accessible with the LHC. The ongoing development of the most important components will facilitate an informed decision about the project, expected around 2015 when the first luminous results from the increased energy LHC become available. In order to then proceed, the whole project is being further developed, which jointly regards its physics, simulation, the detector design as well as the interaction region, civil engineering and many aspects of the accelerator.

During 2012 discussions have gained in intensity at CERN and with(in) the interested community, to evaluate and develop the LHeC prospect, which is uniquely linked to the overriding success and quality of the LHC accelerator. Very recently, CERN has issued a mandate [3] to the LHeC Study Group which is directed to an LHeC ERL test facility and comprises the critical components enabling a decision a few years hence. Since 2006, the LHeC has been part of the EU strategy deliberations, which are now ongoing. The project development has been accompanied by ECFA, the European Committee for Future Accelerators, and by NuPECC, the Nuclear Physics European Collaboration Committee, which in 2010 decided to include the LHeC in its long range plan.

As a new TeV energy scale collider, the LHeC naturally has all the characteristics of a global project of interest and importance extending beyond Europe. Its physics will substantially enrich the LHC programme, to which it represents an upgrade, and its technology is fascinating in many respects. With the addition of an electron beam, CERN would provide the world particle physics community with the counterpart to HERA, which played such a crucial role together with the Tevatron and LEP machines. The LHeC presents a unique opportunity for utilising deep inelastic scattering in the exploration of energy frontier physics, which promises to rewrite our understanding of high density proton and nuclear dynamics and structure.

## References

- [1] J. L. Abelleira Fernandez *et al.* [LHeC Study Group], “A Large Hadron Electron Collider at CERN” J.Phys.G. **39**(2012)075001, arXiv:1206.2913.
- [2] CERN-ECFA-NuPECC Workshop on the LHeC, Chavannes, Switzerland, June 2012, see [http : //cern.ch/lhec](http://cern.ch/lhec).
- [3] S.Bertolucci, Talk at the CERN-ECFA-NuPECC Workshop at Chavannes, Switzerland, see [2].
- [4] S. S. AbdusSalam, B. C. Allanach, H. K. Dreiner, J. Ellis, U. Ellwanger, J. Gunion, S. Heinemeyer and M. Kraemer *et al.*, Eur. Phys. J. C **71** (2011) 1835 [arXiv:1109.3859 [hep-ph]].
- [5] A. Denner, S. Heinemeyer, I. Puljak, D. Rebuzzi and M. Spira, Eur. Phys. J. C **71** (2011) 1753 [arXiv:1107.5909 [hep-ph]].



# LHeC Study Group

J.L.Abelles Fernandez<sup>16,23</sup>, C.Adolphsen<sup>57</sup>, P.Adzic<sup>74</sup>, A.N.Akay<sup>03</sup>, H.Aksakal<sup>39</sup>, J.L.Albacete<sup>52</sup>, B.Allanach<sup>73</sup>, S.Alekhin<sup>17,54</sup>, P.Allport<sup>24</sup>, V.Andreev<sup>34</sup>, R.B.Appleby<sup>14,30</sup>, E.Arikan<sup>39</sup>, N.Armento<sup>53,a</sup>, G.Azelos<sup>33,64</sup>, M.Bai<sup>37</sup>, D.Barber<sup>14,17,24</sup>, J.Bartels<sup>18</sup>, O.Behnke<sup>17</sup>, J.Behr<sup>17</sup>, A.S.Belyaev<sup>15,56</sup>, I.Ben-Zvi<sup>37</sup>, N.Bernard<sup>25</sup>, S.Bertolucci<sup>16</sup>, S.Bettoni<sup>16</sup>, S.Biswal<sup>41</sup>, J.Blümlein<sup>17</sup>, H.Böttcher<sup>17</sup>, A.Bogacz<sup>36</sup>, C.Bracco<sup>16</sup>, J.Bracinik<sup>06</sup>, G.Brandt<sup>44</sup>, H.Braun<sup>65</sup>, S.Brodsky<sup>57,b</sup>, O.Brüning<sup>16</sup>, E.Bulyak<sup>12</sup>, A.Buniatyan<sup>17</sup>, H.Burkhardt<sup>16</sup>, I.T.Cakir<sup>02</sup>, O.Cakir<sup>01</sup>, R.Calaga<sup>16</sup>, A.Caldwell<sup>70</sup>, V.Cetinkaya<sup>01</sup>, V.Chekelian<sup>70</sup>, E.Ciapala<sup>16</sup>, R.Ciftci<sup>01</sup>, A.K.Ciftci<sup>01</sup>, B.A.Cole<sup>38</sup>, J.C.Collins<sup>48</sup>, O.Dadoun<sup>42</sup>, J.Dainton<sup>24</sup>, A.De.Roeck<sup>16</sup>, D.d'Enterria<sup>16</sup>, P.DiNezza<sup>72</sup>, A.Dudarev<sup>16</sup>, A.Eide<sup>60</sup>, R.Enberg<sup>63</sup>, E.Eroglu<sup>62</sup>, K.J.Eskola<sup>21</sup>, L.Favart<sup>08</sup>, M.Fitterer<sup>16</sup>, S.Forte<sup>32</sup>, A.Gaddi<sup>16</sup>, P.Gambino<sup>59</sup>, H.García Morales<sup>16</sup>, T.Gehrmann<sup>69</sup>, P.Gladikh<sup>12</sup>, C.Glasman<sup>28</sup>, A.Glazov<sup>17</sup>, R.Godbole<sup>35</sup>, B.Goddard<sup>16</sup>, T.Greenshaw<sup>24</sup>, A.Guffanti<sup>13</sup>, V.Guzey<sup>19,36</sup>, C.Gwenlan<sup>44</sup>, T.Han<sup>50</sup>, Y.Hao<sup>37</sup>, F.Haug<sup>16</sup>, W.Herr<sup>16</sup>, A.Hervé<sup>27</sup>, B.J.Holzer<sup>16</sup>, M.Ishitsuka<sup>58</sup>, M.Jacquet<sup>42</sup>, B.Jeanneret<sup>16</sup>, E.Jensen<sup>16</sup>, J.M.Jimenez<sup>16</sup>, J.M.Jowett<sup>16</sup>, H.Jung<sup>17</sup>, H.Karadeniz<sup>02</sup>, D.Kayran<sup>37</sup>, A.Kilic<sup>62</sup>, K.Kimura<sup>58</sup>, R.Klees<sup>75</sup>, M.Klein<sup>24</sup>, U.Klein<sup>24</sup>, T.Kluge<sup>24</sup>, F.Kocak<sup>62</sup>, M.Korostelev<sup>24</sup>, A.Kosmicki<sup>16</sup>, P.Kostka<sup>17</sup>, H.Kowalski<sup>17</sup>, M.Kraemer<sup>75</sup>, G.Kramer<sup>18</sup>, D.Kuchler<sup>16</sup>, M.Kuze<sup>58</sup>, T.Lappi<sup>21,c</sup>, P.Laycock<sup>24</sup>, E.Levichev<sup>40</sup>, S.Levonian<sup>17</sup>, V.N.Litvinenko<sup>37</sup>, A.Lombardi<sup>16</sup>, J.Maeda<sup>58</sup>, C.Marquet<sup>16</sup>, B.Mellado<sup>27</sup>, K.H.Mess<sup>16</sup>, A.Milanese<sup>16</sup>, J.G.Milhano<sup>76</sup>, S.Moch<sup>17</sup>, I.I.Morozov<sup>40</sup>, Y.Muttoni<sup>16</sup>, S.Myers<sup>16</sup>, S.Nandi<sup>55</sup>, Z.Nergiz<sup>39</sup>, P.R.Newman<sup>06</sup>, T.Omor<sup>61</sup>, J.Osborne<sup>16</sup>, E.Paoloni<sup>49</sup>, Y.Papaphilippou<sup>16</sup>, C.Pascaud<sup>42</sup>, H.Paukkunen<sup>53</sup>, E.Perez<sup>16</sup>, T.Pieloni<sup>21</sup>, E.Pilicer<sup>62</sup>, B.Pire<sup>45</sup>, R.Placakyte<sup>17</sup>, A.Polini<sup>07</sup>, V.Ptitsyn<sup>37</sup>, Y.Pupkov<sup>40</sup>, V.Radescu<sup>17</sup>, S.Raychaudhuri<sup>35</sup>, L.Rinolfi<sup>16</sup>, E.Rizvi<sup>71</sup>, R.Rohini<sup>35</sup>, J.Rojo<sup>16,31</sup>, S.Russenschuck<sup>16</sup>, M.Sahin<sup>03</sup>, C.A.Salgado<sup>53,a</sup>, K.Sampe<sup>58</sup>, R.Sassot<sup>09</sup>, E.Sauvan<sup>04</sup>, M.Schaefer<sup>75</sup>, U.Schneekloth<sup>17</sup>, T.Schörner-Sadenius<sup>17</sup>, D.Schulte<sup>16</sup>, A.Senol<sup>22</sup>, A.Seryi<sup>44</sup>, P.Sievers<sup>16</sup>, A.N.Skrinsky<sup>40</sup>, W.Smith<sup>27</sup>, D.South<sup>17</sup>, H.Spiesberger<sup>29</sup>, A.M.Stasto<sup>48,d</sup>, M.Strikman<sup>48</sup>, M.Sullivan<sup>57</sup>, S.Sultansoy<sup>03,e</sup>, Y.P.Sun<sup>57</sup>, B.Surrow<sup>11</sup>, L.Szymanowski<sup>66,f</sup>, P.Tael<sup>05</sup>, I.Tapan<sup>62</sup>, T.Tasci<sup>22</sup>, E.Tassi<sup>10</sup>, H.Ten.Kate<sup>16</sup>, J.Terron<sup>28</sup>, H.Thiesen<sup>16</sup>, L.Thompson<sup>14,30</sup>, P.Thompson<sup>06</sup>, K.Tokushuku<sup>61</sup>, R.Tomás García<sup>16</sup>, D.Tommasini<sup>16</sup>, D.Trbojevic<sup>37</sup>, N.Tsoupas<sup>37</sup>, J.Tuckmantel<sup>16</sup>, S.Turkoz<sup>01</sup>, T.N.Trinh<sup>47</sup>, K.Tywoniu<sup>26</sup>, G.Unei<sup>20</sup>, T.Ullrich<sup>37</sup>, J.Urakawa<sup>61</sup>, P.VanMechelen<sup>05</sup>, A.Variola<sup>52</sup>, R.Veness<sup>16</sup>, A.Vivoli<sup>16</sup>, P.Vobly<sup>40</sup>, J.Wagner<sup>66</sup>, R.Wallny<sup>68</sup>, S.Wallon<sup>43,46,f</sup>, G.Watt<sup>69</sup>, C.Weiss<sup>36</sup>, U.A.Wiedemann<sup>16</sup>, U.Wienands<sup>57</sup>, F.Willeke<sup>37</sup>, B.-W.Xiao<sup>48</sup>, V.Yakimenko<sup>37</sup>, A.F.Zarnecki<sup>67</sup>, Z.Zhang<sup>42</sup>, F.Zimmermann<sup>16</sup>, R.Zlebcik<sup>51</sup>, F.Zomer<sup>42</sup>

- <sup>01</sup> *Ankara University, Turkey*
- <sup>02</sup> *SANAEM Ankara, Turkey*
- <sup>03</sup> *TOBB University of Economics and Technology, Ankara, Turkey*
- <sup>04</sup> *LAPP, Annecy, France*
- <sup>05</sup> *University of Antwerp, Belgium*
- <sup>06</sup> *University of Birmingham, UK*
- <sup>07</sup> *INFN Bologna, Italy*
- <sup>08</sup> *IIHE, Université Libre de Bruxelles, Belgium, supported by the FNRS*
- <sup>09</sup> *University of Buenos Aires, Argentina*
- <sup>10</sup> *INFN Gruppo Collegato di Cosenza and Università della Calabria, Italy*
- <sup>11</sup> *Massachusetts Institute of Technology, Cambridge, USA*
- <sup>12</sup> *Charkow National University, Ukraine*
- <sup>13</sup> *University of Copenhagen, Denmark*
- <sup>14</sup> *Cockcroft Institute, Daresbury, UK*
- <sup>15</sup> *Rutherford Appleton Laboratory, Didcot, UK*
- <sup>16</sup> *CERN, Geneva, Switzerland*
- <sup>17</sup> *DESY, Hamburg and Zeuthen, Germany*
- <sup>18</sup> *University of Hamburg, Germany*
- <sup>19</sup> *Hampton University, USA*
- <sup>20</sup> *University of California, Irvine, USA*
- <sup>21</sup> *University of Jyväskylä, Finland*
- <sup>22</sup> *Kastamonu University, Turkey*
- <sup>23</sup> *EPFL, Lausanne, Switzerland*
- <sup>24</sup> *University of Liverpool, UK*
- <sup>25</sup> *University of California, Los Angeles, USA*
- <sup>26</sup> *Lund University, Sweden*
- <sup>27</sup> *University of Wisconsin-Madison, USA*
- <sup>28</sup> *Universidad Autónoma de Madrid, Spain*
- <sup>29</sup> *University of Mainz, Germany*
- <sup>30</sup> *The University of Manchester, UK*
- <sup>31</sup> *INFN Milano, Italy*
- <sup>32</sup> *University of Milano, Italy*
- <sup>33</sup> *University of Montréal, Canada*
- <sup>34</sup> *LPI Moscow, Russia*
- <sup>35</sup> *Tata Institute, Mumbai, India*
- <sup>36</sup> *Jefferson Lab, Newport News, VA 23606, USA*
- <sup>37</sup> *Brookhaven National Laboratory, New York, USA*
- <sup>38</sup> *Columbia University, New York, USA*
- <sup>39</sup> *Nigde University, Turkey*

- 40 *Budker Institute of Nuclear Physics SB RAS, Novosibirsk, 630090 Russia*
- 41 *Orissa University, India*
- 42 *LAL, Orsay, France*
- 43 *Laboratoire de Physique Théorique, Université Paris XI, Orsay, France*
- 44 *University of Oxford, UK*
- 45 *CPHT, École Polytechnique, CNRS, 91128 Palaiseau, France*
- 46 *UPMC University of Paris 06, Faculté de Physique, Paris, France*
- 47 *LPNHE University of Paris 06 and 07, CNRS/IN2P3, 75252 Paris, France*
- 48 *Pennsylvania State University, USA*
- 49 *University of Pisa, Italy*
- 50 *University of Pittsburgh, USA*
- 51 *Charles University, Praha, Czech Republic*
- 52 *IPhT Saclay, France*
- 53 *University of Santiago de Compostela, Spain*
- 54 *Serpukhov Institute, Russia*
- 55 *University of Siegen, Germany*
- 56 *University of Southampton, UK*
- 57 *SLAC National Accelerator Laboratory, Stanford, USA*
- 58 *Tokyo Institute of Technology, Japan*
- 59 *University of Torino and INFN Torino, Italy*
- 60 *NTNU, Trondheim, Norway*
- 61 *KEK, Tsukuba, Japan*
- 62 *Uludag University, Turkey*
- 63 *Uppsala University, Sweden*
- 64 *TRIUMF, Vancouver, Canada*
- 65 *Paul Scherrer Institute, Villigen, Switzerland*
- 66 *National Center for Nuclear Research (NCBJ), Warsaw, Poland*
- 67 *University of Warsaw, Poland*
- 68 *ETH Zurich, Switzerland*
- 69 *University of Zurich, Switzerland*
- 70 *Max Planck Institute Werner Heisenberg, Munich, Germany*
- 71 *QMW University London, United Kingdom*
- 72 *Laboratori Nazionali di Frascati, INFN, Italy*
- 73 *DAMTP, CMS, University of Cambridge, United Kingdom*
- 74 *University of Belgrade, Serbia*
- 75 *RWTH Aachen University, Germany*
- 76 *Instituto Superior Técnico, Universidade Técnica de Lisboa, Portugal*

<sup>a</sup> supported by European Research Council grant HotLHC ERC-2011-StG-279579 and MiCinn of Spain grants FPA2008-01177, FPA2009-06867-E and Consolider-Ingenio 2010 CPAN CSD2007-00042, Xunta de Galicia grant PGIDIT10PXIB206017PR, and FEDER.

<sup>b</sup> supported by the U.S. Department of Energy, contract DE-AC02-76SF00515.

<sup>c</sup> supported by the Academy of Finland, project no. 141555.

<sup>d</sup> supported by the Sloan Foundation, DOE OJI grant No. DE - SC0002145 and Polish NCN grant DEC-2011/01/B/ST2/03915.

<sup>e</sup> supported by the Turkish Atomic Energy Authority (TAEK).

<sup>f</sup> supported by the P2IO consortium.